Dinamica Strutturale with Matlab

Elaborato di Dinamica Strutturale

Antonio Carotenuto

A.A 2024-2025

Contents

List of Figures

Chapter 1

Exercise 1: Comparison of Modal Analysis Results Obtained with an Analytical Approach and with the FEM Method

1.1 Introduction

The objective of this exercise is to determine the natural frequencies of a structure using both an analytical solution and a numerical one, applying the finite element method (FEM). The analysis focuses on evaluating the accuracy of the numerical solution as a function of the number of nodes adopted for two different structures: a rod and a beam. For both structures, we consider the same geometric, mass, and stiffness properties reported in Table 1.1. The schematic representation is shown in Fig.1.1.

Parameter	Symbol	Value
Beam Length	L	10 m
Young's Modulus	E	210×10^9 Pa
Moment of Inertia	I	8.33×10^{-6} m^4
Material Density	ρ	7800 kg/m^3
Cross-sectional Area	A	0.01 m^2

Table 1.1 Problem data for the simply-supported beam

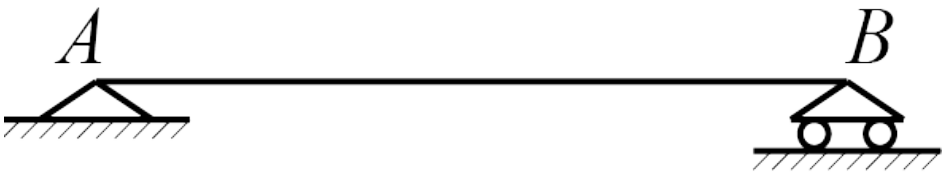

Figure 1.1 Schematic of a simply-supported beam or rod

1.2 Modal Analysis of a Simply-Supported Rod

The natural frequencies of a simply-supported rod can be determined analytically as follows:

$$\omega_n = n\frac{\pi}{L}\sqrt{\frac{E}{\rho}}, \quad n \in \mathbb{N} \tag{1.1}$$

Instead, the FEM solution is based on subdividing the rod into N elements of length L_e. Each element has a stiffness matrix K_e and a mass matrix M_e, both of size 2x2, since each node has only one degree of freedom (longitudinal translation). These elementary stiffness and mass matrices are defined as:

$$K_e = \frac{EA}{L_e}\begin{bmatrix} 1 & -1 \\ -1 & 1 \end{bmatrix} \tag{1.2}$$

$$M_e = \frac{\rho A L_e}{6}\begin{bmatrix} 2 & 1 \\ 1 & 2 \end{bmatrix} \tag{1.3}$$

The MATLAB code that implements the following steps is reported below:

1. **Construction of global matrices**: by assembling the elementary matrices.
2. **Application of boundary conditions**: the rod is supported at both ends, so the nodes at the ends are constrained against translation.
3. **Solution of the eigenvalue problem**: finding the natural frequencies by solving

   $$K\Phi = M\Phi\Lambda \tag{1.4}$$

   from which the natural angular frequencies are obtained

   $$\omega_n = \sqrt{\lambda_n}. \tag{1.5}$$

4. **Comparison with the analytical solution**: calculation of the relative error between the FEM results and the theoretical ones (Fig.1.2-1.3).

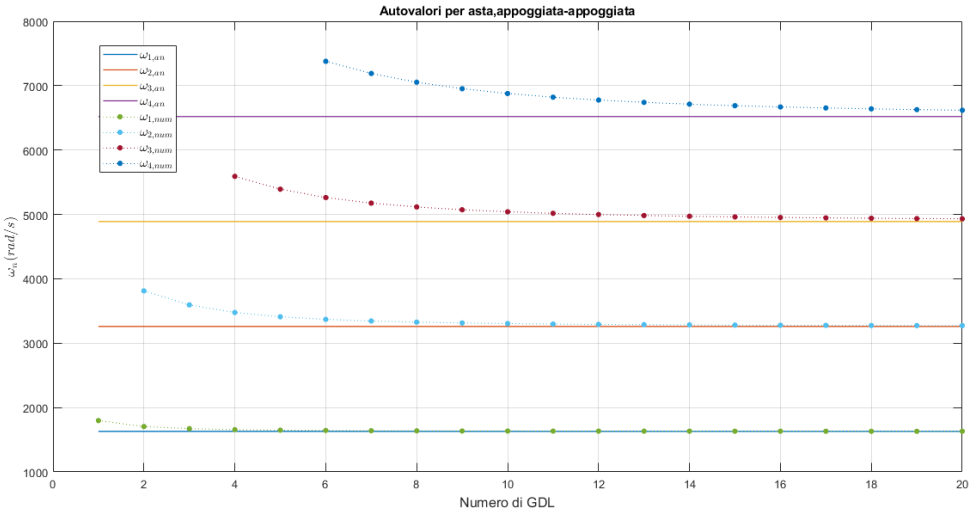

Figure 1.2 Comparison between the first 4 numerical and analytical natural frequencies for the rod

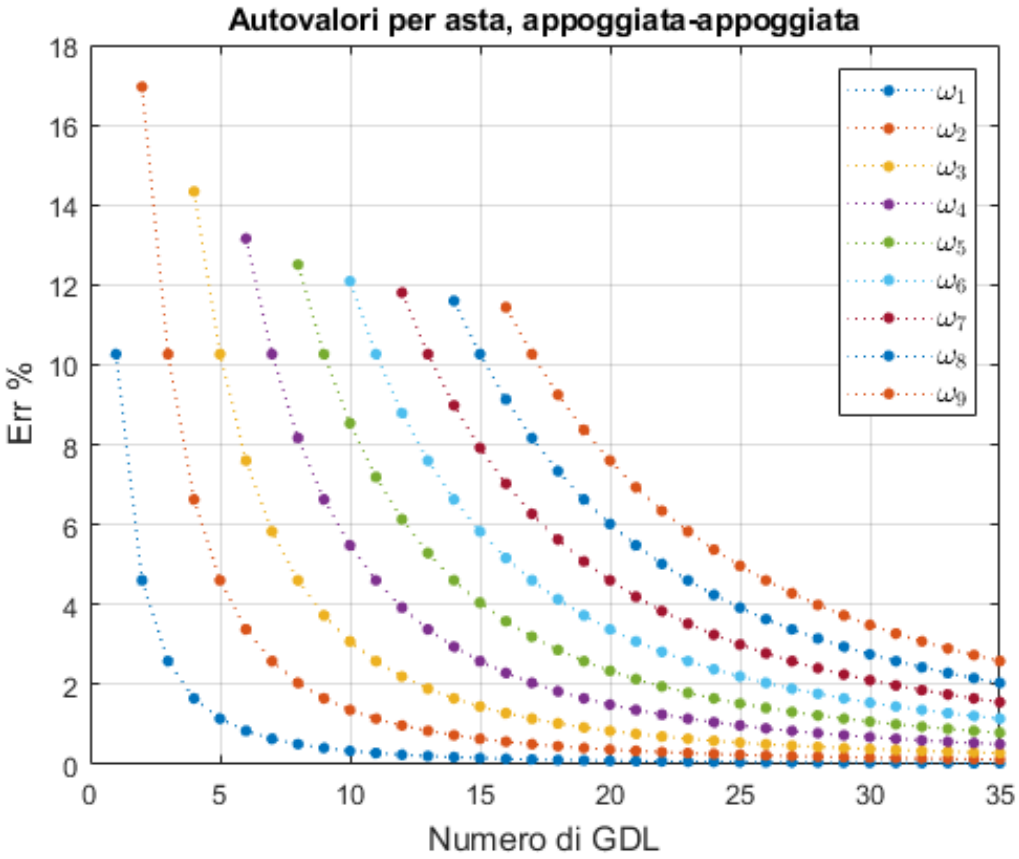

Figure 1.3 Percentage difference evaluated for the first 9 natural frequencies of the rod

Listing 1.1

```
clc;
clear;
close;

%% Informazioni sulla trave
```

```
L = 10;         % Lunghezza della trave (m)
E = 210e9;      % Modulo di Young (Pa)
I = 8.33e-6;    % Momento d'inerzia della sezione (m^4)
rho = 7800;     % Densit  del materiale (kg/m^3)
A = 0.01;       % Area della sezione trasversale (m^2)

%% Soluzione analitica
N_eigen=9;  % Numero di autovalori da calcolare
% Vettore degli indici degli autovalori
a=linspace(1,N_eigen,N_eigen);
% Calcolo delle pulsazioni analitiche
omega_n_vec=a*sqrt(E/rho)*(pi/(L));

%% Soluzione numerica al variare del numero di elementi
l_bound=2;  % Limite inferiore per il numero di elementi
up_bound=36; % Limite superiore per il numero di elementi
N_vec=(l_bound:1:up_bound); % Vettore con il numero di elementi
    considerati
N_free_vec = N_vec-1; % Numero di gradi di libert  liberi
n_it=length(N_vec); % Numero di iterazioni
err=nan(n_it,N_eigen); % Matrice per l'errore relativo
omega_mat=nan(n_it,N_eigen); % Matrice per gli autovalori numerici

for i=1:n_it
    N=N_vec(i); % Numero di elementi
    N_free = N_free_vec(i); % Numero di GDL liberi
    L_el=L/N;  % Lunghezza di un elemento

    % Matrice di rigidezza per un elemento asta
    k_el = (E * A / L_el) * [1, -1; -1, 1];

    % Matrice di massa per un elemento asta (formulazione consistente)
    m_el = (rho * A * L_el / 6) * [2, 1; 1, 2];

    % Inizializzazione delle matrici globali
    K = zeros(N+1, N+1);  % Matrice di rigidezza globale
    M = zeros(N+1, N+1);  % Matrice di massa globale

    % Assemblaggio delle matrici globali
    for p = 1:N
        nodes = [p, p+1];  % Nodi dell'elemento
        K(nodes, nodes) = K(nodes, nodes) + k_el;
        M(nodes, nodes) = M(nodes, nodes) + m_el;
    end

    % Applicazione delle condizioni al contorno
    free_nodes = 2:N; % Nodi liberi (asta vincolata agli estremi)

    % Riduzione del sistema ai soli nodi liberi
    K = K(free_nodes, free_nodes);    % Matrice di rigidezza ridotta
    M = M(free_nodes, free_nodes);    % Matrice di massa ridotta

    % Risoluzione del problema agli autovalori generalizzato
    [Phi, lambda_vec] = eig(K, M);
    lambda_vec=sort(diag(lambda_vec)); % Ordinamento degli autovalori
    lambda_vec=lambda_vec';
```

```
61
62      % Determinazione del numero massimo di autovalori da considerare
63      minim=min(N_eigen,floor((N_free+2)/2));
64
65      % Memorizzazione delle pulsazioni numeriche e calcolo dell'errore
66      omega_mat(i,1:minim) = sqrt(lambda_vec(1:minim));
67      err(i,1:minim) = 100*abs((sqrt(lambda_vec(1:minim))-omega_n_vec(1:
    minim)))./omega_n_vec(1:minim);
68  end
```

1.3 Modal Analysis of a Simply-Supported Beam

The natural frequencies of a simply-supported beam can be determined analytically as follows:

$$\omega_n = \left(\frac{n\pi}{L}\right)^2 \sqrt{\frac{EI}{\rho A}}, \quad \forall n \in \mathbb{N} \tag{1.6}$$

Instead, the FEM solution is based, as in the case of the rod, on subdividing the beam into N elements of length L_e. This time, however, each element has a stiffness matrix $\mathbf{K}_e$ and a mass matrix $\mathbf{M}_e$ of size 4×4, since each node has two degrees of freedom: transverse displacement and rotation.

The elementary stiffness and mass matrices for a beam element are defined as:

$$\mathbf{K}_e = \frac{EI}{L_e^3} \begin{bmatrix} 12 & 6L_e & -12 & 6L_e \\ 6L_e & 4L_e^2 & -6L_e & 2L_e^2 \\ -12 & -6L_e & 12 & -6L_e \\ 6L_e & 2L_e^2 & -6L_e & 4L_e^2 \end{bmatrix} \tag{1.7}$$

$$\mathbf{M}_e = \frac{\rho A L_e}{420} \begin{bmatrix} 156 & 22L_e & 54 & -13L_e \\ 22L_e & 4L_e^2 & 13L_e & -3L_e^2 \\ 54 & 13L_e & 156 & -22L_e \\ -13L_e & -3L_e^2 & -22L_e & 4L_e^2 \end{bmatrix} \tag{1.8}$$

The MATLAB code developed for the analysis implements the same steps seen in the previous section for the rod, and for this reason, it is not reported again. Only the results are reported (Fig.1.4-1.5).

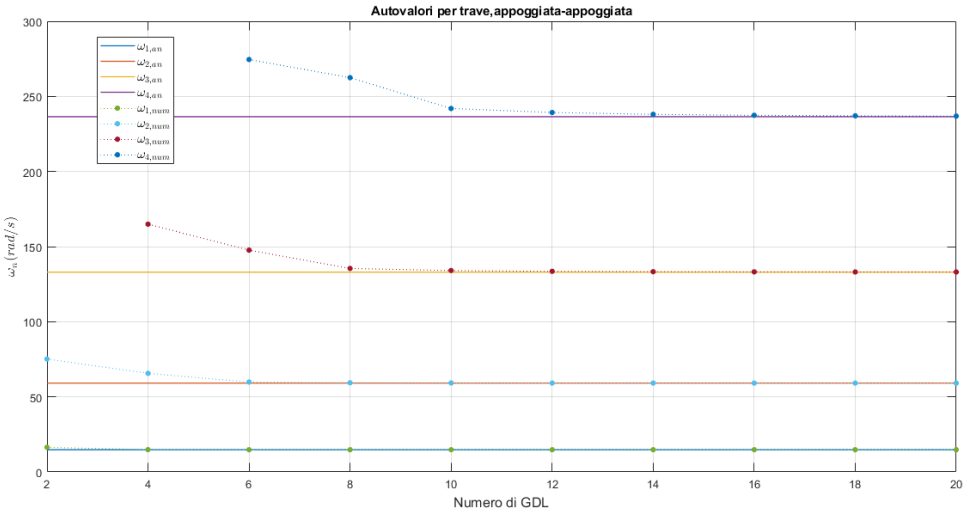

Figure 1.4 Comparison between the first 4 numerical and analytical natural frequencies for the beam

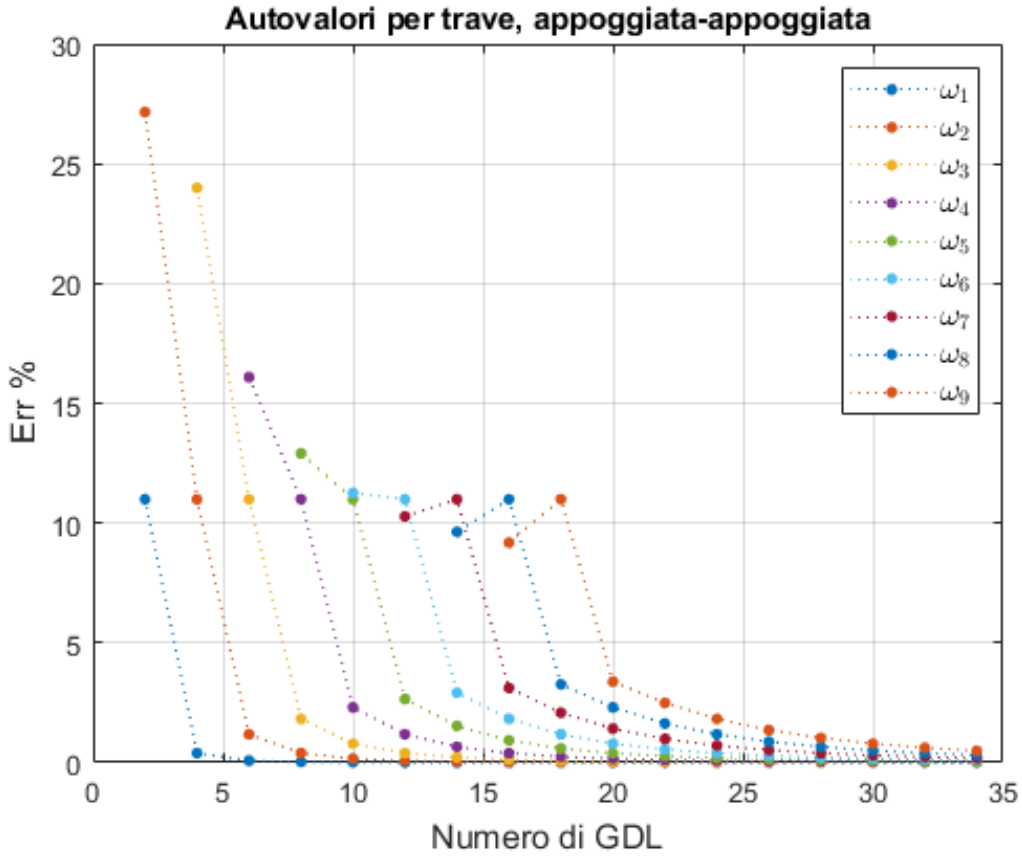

Figure 1.5 Percentage difference evaluated for the first 9 natural frequencies of the beam

1.4 Discussion of the Obtained Results

From Figures 1.2-1.5, it can be observed that:

- the numerical natural frequencies are always higher than the corresponding analytical ones;
- for both the rod and the beam analysis, the numerical frequencies tend towards

those evaluated with an analytical approach as the number of elements increases. This result is not trivial, because the FEM approach with (H) type formulation was used, and therefore the "Inclusion Principle" cannot be applied;

- for a given number of DOFs considered for the numerical solution, the lower natural frequencies are those that are better approximated, also because they are evaluated more times;
- The numerical natural frequencies of the rod tend uniformly to the analytical frequencies, while for the beam frequencies, there is no monotonic trend.

The last observation can be justified by noting that the natural frequencies of the rod are associated with longitudinal vibrations, and these are described by a second-order differential equation in space and a second-order in time, reducible to the wave equation. The frequencies of the beam, however, are associated with flexural vibrations described by a fourth-order differential equation in space and second-order in time, not reducible to the wave equation. This observation leads us to say that even if we use FEM in the (H) formulation for longitudinal vibrations, the "Inclusion Principle" still applies, while for flexural vibrations, this is not true.

Chapter 2

Exercise 2: Modal Characteristics and FRF

2.1 Introduction

The objective of this chapter is to obtain the modal characteristics and frequency response functions of the 3-mass, 6-spring system shown in Fig.2.1, as presented in [**Ewins**]. The stiffness and inertia properties reported in Tab.2.1 are considered, and for this system, 3 damping conditions are examined:

- undamped system;
- proportional hysteretic damping;
- non-proportional hysteretic damping;

.

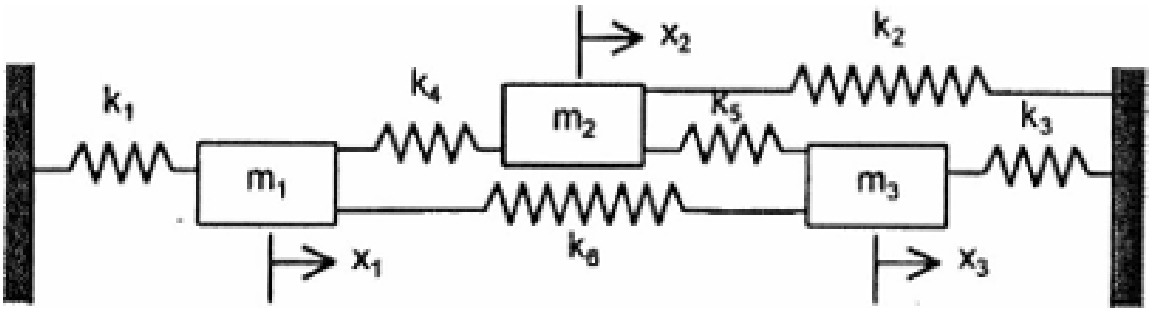

Figure 2.1 System of 3 masses and 6 springs presented in [**Ewins**]

2.2 Eigenvalues and Eigenvectors

The MATLAB code that implements the following steps is reported below:

Parameter	Value
m_1	1.00 kg
m_2	0.95 kg
m_3	1.05 kg
$k_1, k_2, k_3, k_4, k_5, k_6$	1.0×10^3 N/m

Table 2.1 System data

1. **Construction of mass M and stiffness K matrices**: the mass matrix is diagonal because the system has lumped masses; the stiffness matrix is given by the values representing the connection between masses through the springs.

$$M = \begin{bmatrix} m_1 & 0 & 0 \\ 0 & m_2 & 0 \\ 0 & 0 & m_3 \end{bmatrix} = \begin{bmatrix} 1.00 & 0 & 0 \\ 0 & 0.95 & 0 \\ 0 & 0 & 1.05 \end{bmatrix} \tag{2.1}$$

$$K = \begin{bmatrix} k+k+k & -k & -k \\ -k & k+k+k & -k \\ -k & -k & k+k+k \end{bmatrix} = \begin{bmatrix} 3000 & -1000 & -1000 \\ -1000 & 3000 & -1000 \\ -1000 & -1000 & 3000 \end{bmatrix} \tag{2.2}$$

2. **Calculation of eigenvalues and eigenvectors in the undamped case**: The natural frequencies of the system are calculated by solving the eigenvalue problem

$$K\Phi = \lambda M\Phi \tag{2.3}$$

where: λ represents the eigenvalues, i.e., the natural frequencies squared, and Φ represents the associated modes. The eigenvalues are sorted in ascending order, and the eigenvectors are normalized with respect to the mass matrix to ensure consistency. The results are obtained in Fig.2.2-2.3.

LAMBDA_UN

3x3 double

	1	2	3
1	999.4451	0	0
2	0	3.8919e+03	0
3	0	0	4.1237e+03

Figure 2.2 Eigenvalues of the undamped system [**Ewins**]

PHI_UN

3x3 double

	1	2	3
1	-0.5769	-0.6020	0.5521
2	-0.5674	-0.2150	-0.8273
3	-0.5866	0.7519	0.2070

Figure 2.3 Eigenvectors of the undamped system

3. **Proportional damping**: Proportional structural damping is introduced through a coefficient β, which is used to define the damping matrix as:

$$D_1 = \beta K$$

The eigenvalue problem is then solved for the modified matrix $K + jD_1$, where the imaginary term represents the effect of damping. In this case as well, the modal forms are normalized with respect to the mass matrix, and the results are shown in Fig.2.4-2.5.

LAMBDA_PROP_DUMP

3x3 complex double

	1	2	3
1	9.9945e+02 + 4.9972e+01i	0.0000 + 0.0000i	0.0000 + 0.0000i
2	0.0000 + 0.0000i	3.8919e+03 + 1.9460e+02i	0.0000 + 0.0000i
3	0.0000 + 0.0000i	0.0000 + 0.0000i	4.1237e+03 + 2.0618e+02i

Figure 2.4 Eigenvalues of the system with proportional damping

PHI_PROP_DUMP

3x3 complex double

	1	2	3
1	0.5769 + 0.0000i	-0.6020 - 0.0000i	0.5521 - 0.0000i
2	0.5674 + 0.0000i	-0.2150 + 0.0000i	-0.8273 + 0.0000i
3	0.5866 - 0.0000i	0.7519 + 0.0000i	0.2070 - 0.0000i

Figure 2.5 Eigenvectors of the system with proportional damping

4. **Non-proportional damping**: Unlike the previous case, the damping is not proportional to the stiffness. A damping matrix D_2 is defined with a significant value only in the first diagonal component:

$$D_2(1,1) = 0.3k$$

The eigenvalue analysis is repeated for the modified system, including non-proportional damping. Here too, the eigenvectors are normalized. The results are shown in Fig.2.6-2.7.

LAMBDA_NOPROP

3x3 complex double

	1	2	3
1	1.0061e+03 + 9.9609e+01i	0.0000 + 0.0000i	0.0000 + 0.0000i
2	0.0000 + 0.0000i	3.9416e+03 + 1.2149e+02i	0.0000 + 0.0000i
3	0.0000 + 0.0000i	0.0000 + 0.0000i	4.0673e+03 + 7.8900e+01i

Figure 2.6 Eigenvalues of the system with non-proportional damping

	1	2	3
1	0.5762 - 0.0387i	-0.8108 + 0.2580i	0.5236 + 0.4422i
2	0.5687 + 0.0176i	-0.1131 - 0.5587i	-1.0169 + 0.0720i
3	0.5880 + 0.0208i	0.8306 + 0.1710i	0.3603 - 0.4281i

Figure 2.7 Eigenvectors of the system with non-proportional damping

Listing 2.1

```
clc;
clear;
close all;
N = 3; % GDL
m1=1; % Kg
m2=0.95; % Kg
m3=1.05; % Kg

k=1.0e3; % N/m

M=[m1, 0, 0;        % Mass Matrix
    0, m2, 0;
    0, 0, m3];

K=[k+k+k, -k, -k; % Stiffness Matrix
    -k, k+k+k, -k;
    -k, -k, k+k+k];

% %%%%%%%%%%%%%%%%%%%%%%%%%%%%%%%%%%%%%%%%%%%%%%%%%%%%%%%%%%%%%%%%%%%%%%%%%%

%%%%%%%%%%%%%%%%%%%%     UNDAMPED %%%%%%%%%%%%%%%%%%%%%%%%%%%%%%%%%%%%%

[PHI_UN, LAMBDA_UN] = eig(K, M);
[LAMBDA_UN,ind_1]=sort(diag(LAMBDA_UN));
LAMBDA_UN=diag(LAMBDA_UN);
PHI_UN=PHI_UN(:,ind_1);

for i = 1:size(PHI_UN, 2)  % Itera su ogni autovettore
    v = PHI_UN(:, i);  % Estrai l'autovettore i-esimo
    norm_factor = sqrt(v' * M * v);  % Calcola il fattore di normalizzazione
    PHI_UN(:, i) = v / norm_factor;  % Normalizza l'autovettore
end

% %%%%%%%%%%%%%%%%%%%%%%%%%%%%%%%%%%%%%%%%%%%%%%%%%%%%%%%%%%%%%%%%%%%%%%%%%%

%%%%%%%%        PROPORTIONAL STRUCTURAL DAMPING %%%%%%%%%%%%%
beta=0.05;
D_1 = beta*K;
[PHI_PROP_DUMP, LAMBDA_PROP_DUMP] = eig(K+1j*D_1, M);
[LAMBDA_PROP_DUMP,ind_2]=sort(diag(LAMBDA_PROP_DUMP));
```

```
LAMBDA_PROP_DUMP=diag(LAMBDA_PROP_DUMP);
PHI_PROP_DUMP=PHI_PROP_DUMP(:,ind_2);

for i = 1:size(PHI_PROP_DUMP, 2)  % Itera su ogni autovettore
    v = PHI_PROP_DUMP(:, i);  % Estrai l'autovettore i-esimo
    norm_factor = sqrt(v' * M * v);  % Calcola il fattore di normalizzazione
    PHI_PROP_DUMP(:, i) = v / norm_factor;  % Normalizza l'autovettore
end


%%%%%%%%%%%%%%%%%%%%%%%%%%%%%%%%%%%%%%%%%%%%%%%%%%%%%%%%%%%%%%%%%%%%%%%%%%%
%%%%%%%%        NON PROPORTIONAL STRUCTURAL DAMPING %%%%%%%%%
d=0.3*k;
D_2 = zeros(3,3);
D_2(1,1) = d;
[PHI_NOPROP, LAMBDA_NO_PROP] = eig(K+(1j*D_2), M);
[LAMBDA_NO_PROP,ind_3]=sort(diag(LAMBDA_NO_PROP));
LAMBDA_NO_PROP=diag(LAMBDA_NO_PROP);
PHI_NOPROP=PHI_NOPROP(:,ind_3);

for i = 1:size(PHI_NOPROP, 2)  % Itera su ogni autovettore complesso
    v = PHI_NOPROP(:, i);  % Estrai l'autovettore i-esimo
    norm_factor = sqrt(conj(v)' * M * v);  % Normalizzazione Hermitiana
    PHI_NOPROP(:, i) = v / norm_factor;  % Normalizza l'autovettore
end
```

2.2.1 Analysis of Results

From the results shown in Figs.2.2-2.7, we can deduce some interesting information:

- In the case of an undamped structure, both the eigenvalues ($\lambda_r = \bar{\omega}_r^2$) and the eigenvectors ($\bar{\Phi}_r$) are real. Furthermore, it was possible to normalize the eigenvectors with respect to the mass matrix because the eigenvectors possess the property of orthogonality.

- In the case of proportional hysteretic damping, the eigenvalues are complex and are equal to:
$$\lambda_r = \bar{\omega}_r^2 (1 + i\eta_r) \tag{2.4}$$
with $\eta_r = \beta$. The eigenvectors, however, are real and are exactly equal to those of the undamped case (Φ_r=$\bar{\Phi}_r$).

- In the case of non-proportional structural damping, the eigenvalues are complex and can be formally expressed as:
$$\lambda_r = \omega_r^2 (1 + i\eta_r) \tag{2.5}$$
where, however, $\omega_r \neq \bar{\omega}_r$ and $\eta_r \neq \beta$. The eigenvectors are different from those of the undamped system; they are complex, but it can still be shown that they possess the property of orthogonality.

. Fig.2.8 shows the eigenvectors with representation in magnitude and phase. It is observed that in the undamped case and in the case of proportional damping, since the eigenvectors are real, the phase only takes values of 0° or 180°. This means that the different DOFs can only oscillate in phase or in phase opposition. This also implies that the deformed shape of the system always assumes the same form and can be determined with a single snapshot. Conversely, in the case of non-proportional damping, the eigenvectors are complex, and therefore the phases are generally different from 0° or 180°. This implies that the DOFs can be out of phase with each other, and thus we do not always observe the same deformed shape.

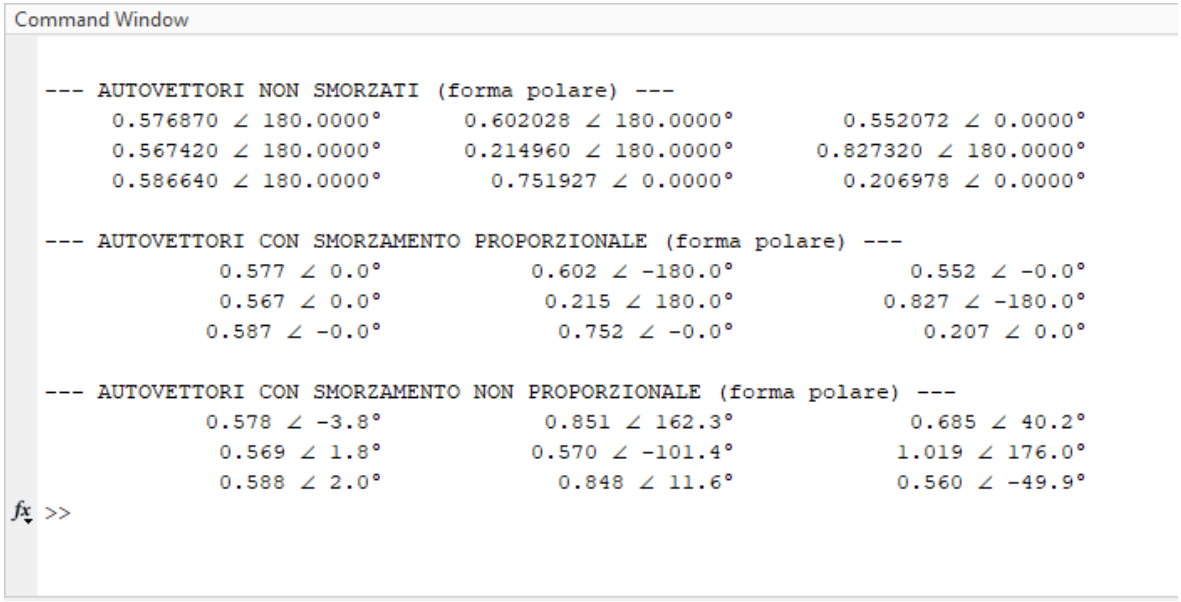

Figure 2.8 Eigenvectors of the system in the three damping cases with magnitude and phase representation

2.3 FRF: Frequency Response Function

The section of the MATLAB script that allows determining the receptance matrix $[\boldsymbol{\alpha}(\omega)]$ for the 3-mass, 6-spring system we are examining is reported below. The elements of the receptance matrix are defined as:

$$\alpha_{j,k}(\omega) = \frac{X_j(\omega)}{F_k(\omega)} \tag{2.6}$$

where $F_k(\omega)$ is the force applied at the k-th DOF and $X_j(\omega)$ is the system's response at the j-th DOF. These are evaluated in the script in 2 different ways:

- In the first case, the receptance matrix is evaluated as follows:

$$[\alpha(\omega)] = \left(\mathbf{K} + j\mathbf{D} - \omega^2\mathbf{M}\right)^{-1} \tag{2.7}$$

  where K, D, and M are the stiffness, damping, and mass matrices as defined in the previous section.

- In the second case, the elements of the matrix are evaluated directly using the following relation:

$$\alpha_{j,k}(\omega) = \sum_{r=1}^{N} \frac{\phi_j^{(r)}\,\phi_k^{(r)}}{\lambda_r - \omega^2} \tag{2.8}$$

  with:

  - $\phi_j^{(r)}$ and $\phi_k^{(r)}$ are the j-th and k-th components of mode r,
  - λ_r is the eigenvalue associated with mode r, i.e., $\lambda_r = \omega_r^2$,
  - ω is the analyzed frequency,
  - N is the total number of modes considered.

It can be observed that not only does the second method allow direct observation of the frequency response's dependence on modal characteristics, but it is also less computationally expensive.

Listing 2.2

```
%%                                                                        %%
% %%%%%%%%%%%%%%%%%%%%%%%%%%%%%%%%%%%%%%%%%%%%%%%%%%%%%%%%%%%%%%%%%%%%%%%%%%
%%%%%%%%%%%%              FRF              %%%%%%%%%%
L = 100000;
omega_max = sqrt(LAMBDA_UN(3,3));
% Range di frequenze per il calcolo della FRF
omega = linspace(0, 1.3*omega_max, L);

% Risposta nel nodo j
j = 3;

% Forza applicata nel nodo i
k = 1;

% Calcolo della FRF per i tre modelli: senza smorzamento, proporzionale,
% non proporzionale
%inizializzo risposte
FRF_UN = zeros(1,L);
FRF_PROP_DUMP = zeros(1,L);
FRF_NO_PROP = zeros(1,L);

FRF_UN_rip = zeros(1,L);
FRF_PROP_DUMP_rip = zeros(1,L);
FRF_NO_PROP_rip = zeros(1,L);

%% Caso senza smorzamento
D_UN = zeros(3, 3);  % Matrice di smorzamento nulla

for i = 1:L
    %% Caso senza smorzamento
    H1 = inv(K+1j*D_UN-((omega(i))^2)*M);
    FRF_UN(i) = H1(j,k);
```

```
33
34
35      %% Caso smorzamento Proporzionale
36      H2 = inv(K+1j*D_1-((omega(i))^2)*M);
37      FRF_PROP_DUMP(i) = H2(j,k);
38
39
40      %% Caso smorzamento non proporzionale
41      H3 = inv(K+1j*D_2-((omega(i))^2)*M);
42      FRF_NO_PROP(i) = H3(j,k);
43  end
44
45  for r=1:N
46  %% Caso senza smorzamento
47    FRF_UN_rip = FRF_UN_rip+((PHI_UN(j,r)*PHI_UN(k,r))./...
48          (LAMBDA_UN(r,r)-(omega.^2)));
49  %% Caso smorzamento Proporzionale
50    FRF_PROP_DUMP_rip = FRF_PROP_DUMP_rip+...
51        ((PHI_PROP_DUMP(j,r)*PHI_PROP_DUMP(k,r))./...
52          (LAMBDA_PROP_DUMP(r,r)-(omega.^2)));
53  %% Caso smorzamento non proporzionale
54    FRF_NO_PROP_rip = FRF_NO_PROP_rip+((PHI_NOPROP(j,r)*PHI_NOPROP(k,r))
      ./...
55          (LAMBDA_NO_PROP(r,r)-(omega.^2)));
56  end
```

2.3.1 Results

For brevity, plots of only two frequency responses are reported:

- the cross-receptance function $\alpha_{1,3}(\omega)$ (Fig.2.9)
- the direct-receptance function $\alpha_{1,1}(\omega)$ (Fig.2.10)

for the three different damping conditions. From the results, we can observe that:

- for ω approaching 0, the response coincides with the static response;
- in the undamped system case, the response increases around the resonance frequencies up to divergence;
- in the damped case, the response increases near resonance but does not diverge, reaching a maximum point, which does not correspond to the natural frequency point of the undamped system;
- since the resonance frequencies ω_2 and ω_3 are very close to each other, it is possible to distinguish 2 distinct peaks by eye only in the undamped system case;
- the main property that characterizes the direct-receptance function compared to the cross-receptance is the presence of anti-resonances: between 2 resonance frequencies, a point is observed where the response can be considered engineeringly null.
- it is also observed from Fig.2.11 that in the undamped case (the same can be said in general for a very lightly damped case), the accuracy with which one can evaluate the response near resonance is very strongly influenced by the frequency step considered.

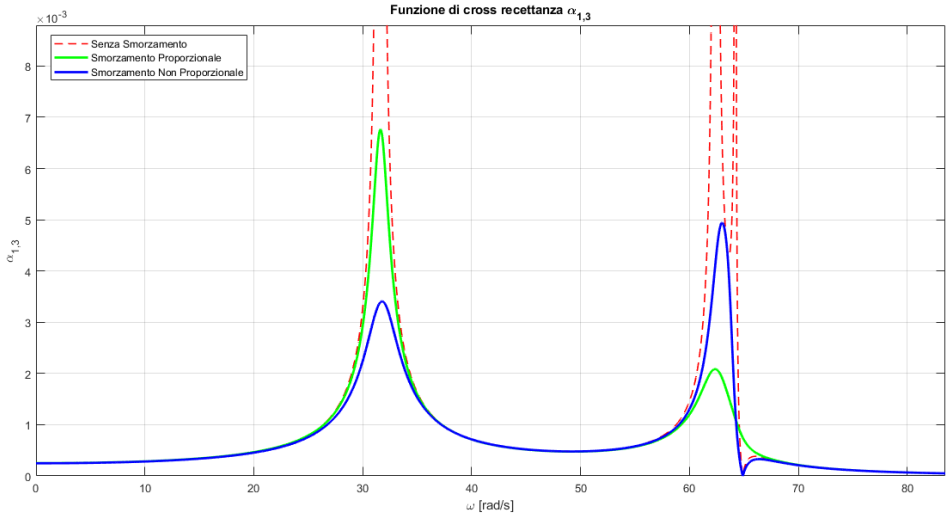

Figure 2.9 Cross-receptance function $\alpha_{1,3}$

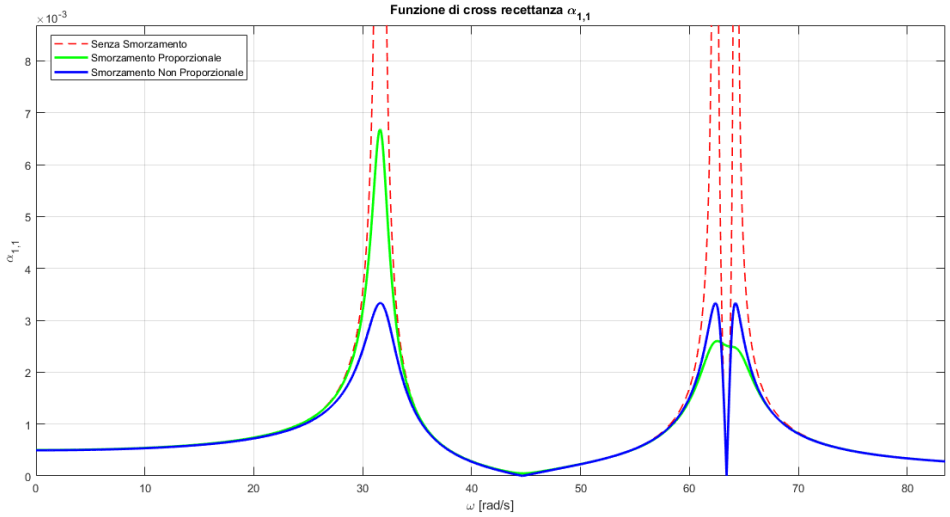

Figure 2.10 Direct-receptance function $\alpha_{1,1}$

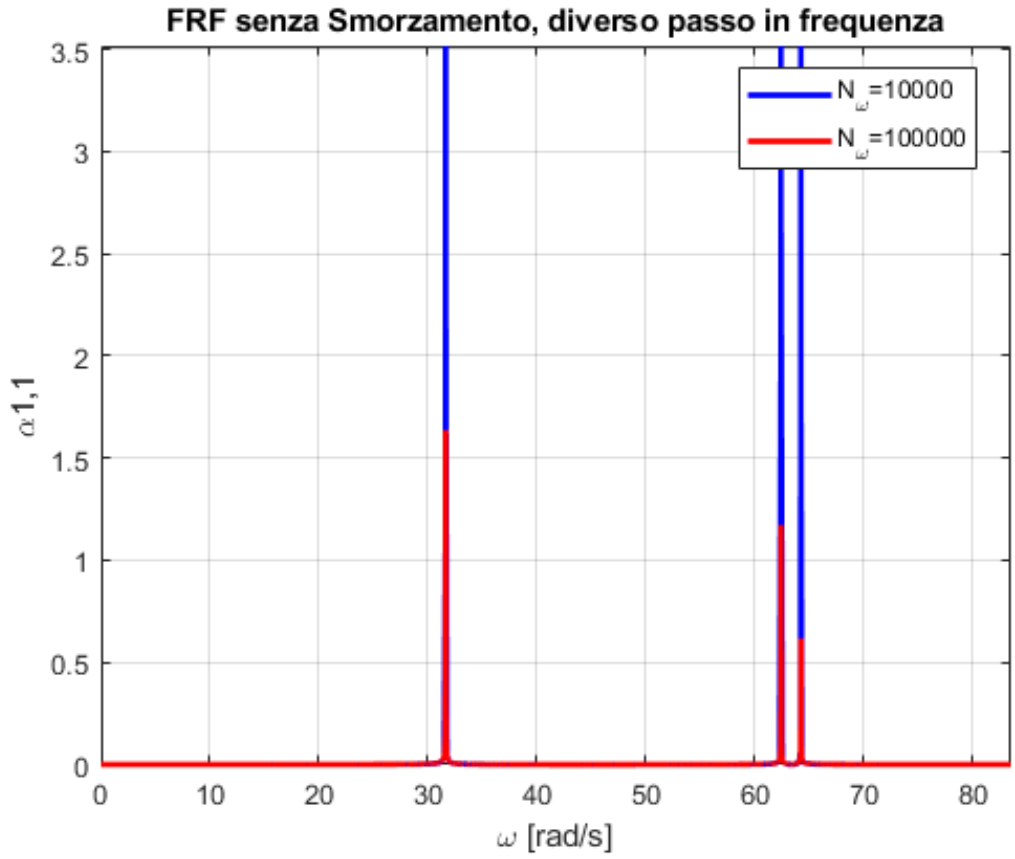

Figure 2.11 Effect of frequency step variation

Bibliography

[1] D. J. Ewins, *Modal Testing: Theory, Practice and Application*, 2nd ed., Research Studies Press Ltd, 2000.

Chapter 3

Exercise 3: Extraction of Modal Information using the Circle-Fit Technique

3.1 Introduction

In the first chapter, it was shown how to obtain the spatial properties (mass matrix and stiffness matrix) of a beam with specific boundary conditions using the FEM approach. In the second chapter, however, it was observed how to obtain modal information and FRFs for a certain numerical model representative of a simple system with different damping conditions. In this chapter, these notions are used to construct an FEM numerical model for a beam with properties reported in Tab.3.2, considering a beam made up of N=14 elements. The beam is assumed to be simply-supported and with proportional hysteretic damping with $\beta = 0.05$. The modal information (frequencies, damping, and modes) was determined, and finally, a receptance function was reconstructed. For the following reasoning, the function $\alpha_{3,3}(\omega)$ reported in Fig.3.1 was chosen. At this point, we proceed with the hypothesis that the FRF thus obtained is the result of an experimental acquisition. Therefore, the circle-fit technique is used to reconstruct the resonance frequencies, damping ratios, and modal constants. These results can then be compared with the pseudo-experimental database (Tab.3.1). It is decided to use the SDOF modal extraction technique on the first 3 peaks as they are considered sufficiently separated from each other (Fig.3.2).

Table 3.1 Estimated modal parameters for the first three modes

Mode r	Frequency ω_r [rad/s]	Damping η_r	Modal Constant ${}_rA_{3,3}$
1	14.7804	0.05	2.4054×10^{-4}
2	59.1230	0.05	8.2179×10^{-4}
3	133.0418	0.05	1.4000×10^{-3}

Parameter	Symbol	Value
Beam Length	L	10 m
Young's Modulus	E	210×10^9 Pa
Moment of Inertia	I	8.33×10^{-6} m^4
Material Density	ρ	7800 kg/m^3
Cross-sectional Area	A	0.01 m^2

Table 3.2 Problem data for the simply-supported beam

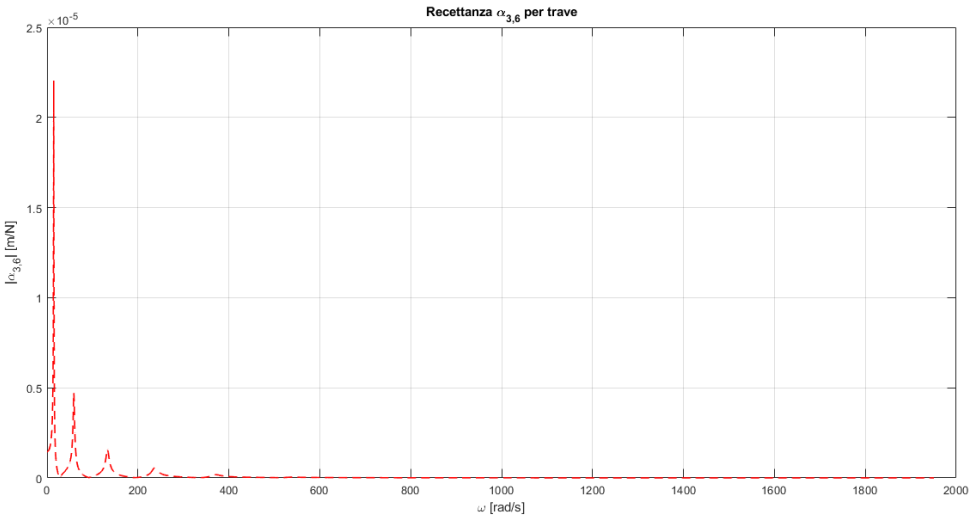

Figure 3.1 Receptance function $\alpha_{3,3}$ for a simply-supported beam

3.2 Procedure for Modal Parameter Extraction

This section describes the procedure used to estimate the modal damping coefficient η_r, the resonance frequency ω_r, and the modal constant ${}_rA_{j,k}$, $through a circle fit in the complex plane of the$

- The complex FRF, previously calculated, is analyzed to identify resonance peaks. For this purpose, a basic `peak-picking` function is used, which detects local maxima in the FRF magnitude.
- A frequency interval centered on ω_{res} equal to ±10% of its value is selected:

$$\omega_{\text{fit}} \in [0.9\omega_{\text{peak}},\ 1.1\omega_{\text{peak}}]. \tag{3.1}$$

  The corresponding portion of the complex FRF is then extracted.
- The real and imaginary parts of the FRF are used to fit a circle in the complex plane. The equation of the circle is:

$$(x - x_c)^2 + (y - y_c)^2 = R^2, \tag{3.2}$$

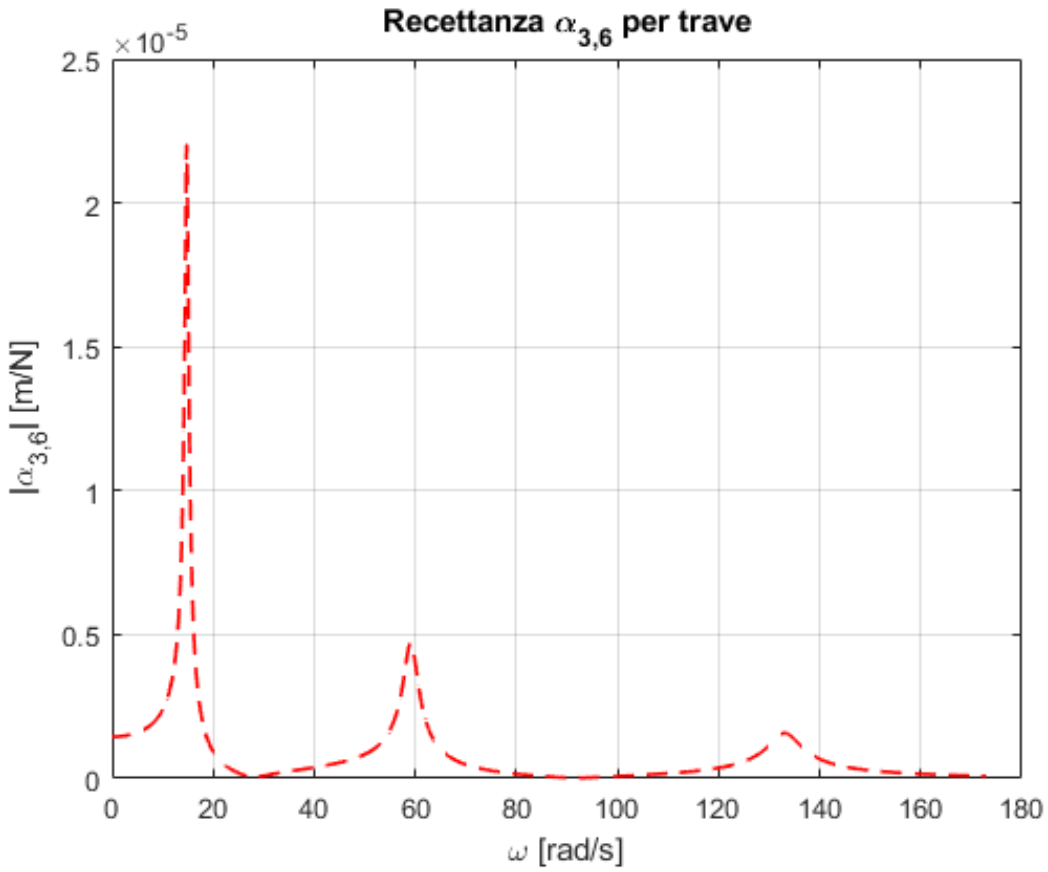

Figure 3.2 Zoomed receptance function $\alpha_{3,3}$ for a simply-supported beam around resonances

which can be rewritten in matrix form as:

$$\begin{bmatrix} -2x & -2y & 1 \end{bmatrix} \begin{bmatrix} x_c \\ y_c \\ C \end{bmatrix} = -(x^2 + y^2).$$

The solution is obtained using a least squares method:

$$\mathbf{A} \cdot \mathbf{p} = \mathbf{b}, \quad \text{where } \mathbf{p} = \begin{bmatrix} x_c \\ y_c \\ C \end{bmatrix}.$$

Once the center (x_c, y_c) and C are obtained, the radius is calculated:

$$R = \sqrt{x_c^2 + y_c^2 - C}.$$

- The resonance frequency is then evaluated using 3 different methods: the frequency at which the imaginary part of the receptance has its maximum value; the frequency at which the real part is zero; the frequency at which the FRF magnitude is maximum.
- The damping is calculated as:

$$\eta_r = \frac{\omega_a - \omega_b}{\omega_r}$$

where ω_a and ω_b are the points on the horizontal diameter of the circle;

- the modal constants were determined in magnitude using the following method:

$$ {}_rA_{j,k} = 2R \cdot \omega_r^2 \cdot \eta_r $$

- since the damping is of proportional hysteretic type, it is assumed that the modal constants are real.

Listing 3.1

```
%% ========================================================================

%                   STIMA FREQUENZA NATURALE (CIRCLE FIT)
%
    ========================================================================

[pks, locs] = findpeaks_basic(abs(FRF_PROP_DUMP));
peak_idx = locs(3);  % Terza risonanza
w_res = omega(peak_idx);

% Intervallo per interpolazione
window_pct = 0.1;
intorno = find(omega > (1-window_pct)*w_res & omega < (1+window_pct)*
    w_res);
omega_fit = omega(intorno);
FRF_fit = FRF_PROP_DUMP(intorno);

% Circle fit nel piano complesso
x = real(FRF_fit);
x = x(:);
y = imag(FRF_fit);
y = y(:);
A = [-2*x, -2*y, ones(length(x),1)];
b = -(x.^2 + y.^2);
params = A\b;

xc = params(1); yc = params(2);
R = sqrt(xc^2 + yc^2 - params(3));
D = 2 * R;
C = xc + 1i*yc;

% Interpolazione spline complessa
FRF_spline = @(w) interp1(omega_fit, FRF_fit, w, 'spline');

omega_n_1 = fminbnd(@(w) imag(FRF_spline(w)), omega_fit(1), omega_fit(end
    ));
omega_n_2 = fzero(@(w) real(FRF_spline(w)), w_res);
omega_n_3 = fminbnd(@(w) -abs(FRF_spline(w)), omega_fit(1), omega_fit(end
    ));

z1 = FRF_spline(omega_n_1);
z2 = FRF_spline(omega_n_2);
z3 = FRF_spline(omega_n_3);
```

```
38
39 % Stampa risultati frequenze naturali
40 fprintf('\n=== Frequenze naturali stimate sulla circle fit ===\n');
41 fprintf('Metodo 1 (max Im):              = %.4f rad/s\n', omega_n_1);
42 fprintf('Metodo 2 (Re = 0):              = %.4f rad/s\n', omega_n_2);
43 fprintf('Metodo 3 (max |FRF|):           = %.4f rad/s\n', omega_n_3);
44
45 %% ========================================================================
46 %                    STIMA SMORZAMENTO MODALE
47 % ========================================================================
48 FRF_shifted = FRF_fit - C;
49 theta_FRF = unwrap(angle(FRF_shifted));
50
51 omega_a = interp1(theta_FRF, omega_fit, 0, 'linear');
52 omega_b = interp1(theta_FRF, omega_fit, -pi, 'linear');
53
54 zeta = (omega_a - omega_b) / omega_n_1;
55
56 fprintf('\nomega_a (   = 0):    %.4f rad/s\n', omega_a);
57 fprintf('omega_b (   =   ):    %.4f rad/s\n', omega_b);
58 fprintf('Smorzamento stimato:          = %.4f\n', zeta);
59
60 % Costante modale stimata
61 A33_1 = 2 * R * (omega_n_1^2) * zeta;
62 fprintf('\nDiametro:   D = %f\n', D);
63 fprintf('Costante modale stimata:    A      ,    = %f\n', A33_1);
```

3.3 Discussion of Results

Figures 3.3-3.8 report the circle-fit results, and we can observe that:

- as expected, since there is structural type damping and because the peaks are sufficiently isolated from each other, the receptance function in the complex plane can be easily approximated with a circle that has its center almost on the imaginary axis and is almost entirely in the negative imaginary semi-plane.
- since the system is actually MDOF, the circle is not exactly what we would have had in the SDOF case, and it is not possible to describe all 360°.
- the study is done with a constant frequency step, and therefore it can be observed that, approaching the resonance frequency, the same frequency jump corresponds to a larger jump in the angular position θ.
- the frequencies evaluated with the three different methods are almost identical.
- the phase of the modal constants should be either 0° or 180°; if this were the case, the principal diameter would be parallel to the real axis. This is not exactly true, which is due to numerical error.

- the error committed, as expected, is practically nil in the extraction of modal parameters, given the small frequency step and especially since the data used are pseudo-experimental and therefore not affected by error.
- the frequency at which the FRF assumes maximum magnitude is the one that best approximates the reference one and was chosen to evaluate the goodness of the results and for the damping ratios.

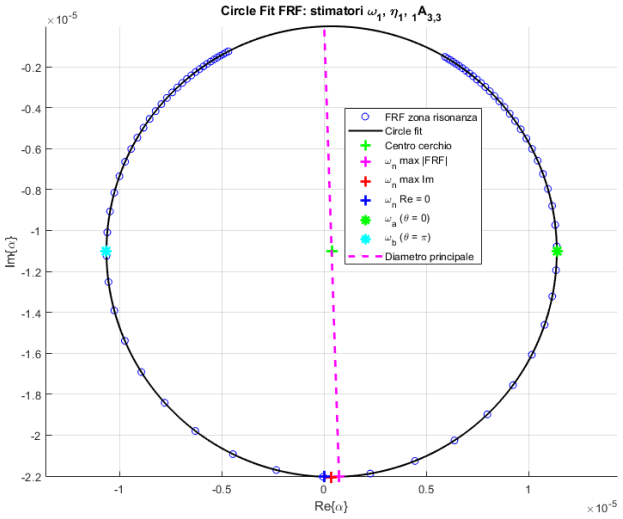

Figure 3.3 Circle-fit for the receptance function around the first peak

```
=== Frequenze naturali stimate sulla circle fit ===
Metodo 1 (max Im):        ω1 = 14.7804 rad/s
Metodo 2 (Re = 0):        ω1  = 14.7865 rad/s
Metodo 3 (max |FRF|):     ω1n  = 14.7743 rad/s

omega_a (θ = 0):     14.4058 rad/s  [destra del cerchio]
omega_b (θ = π):     15.1456 rad/s  [sinistra del cerchio]
Smorzamento stimato:     η1 = -0.0501

Diametro:    D = 0.000022
Costante modale stimata:     1A3,3 = -0.000241
>>
```

Figure 3.4 Results for the first modal component

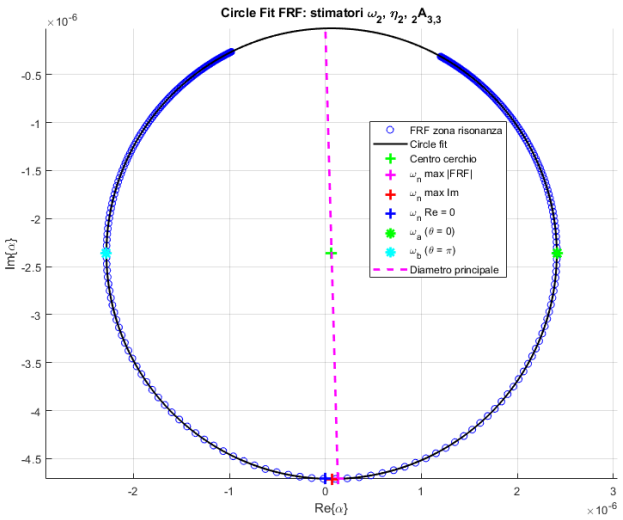

Figure 3.5 Circle-fit for the receptance function around the second peak

```
=== Frequenze naturali stimate sulla circle fit ===
Metodo 1 (max Im):        ω2 = 59.1231 rad/s
Metodo 2 (Re = 0):        ω2  = 59.1434 rad/s
Metodo 3 (max |FRF|):     ω2  = 59.1028 rad/s

omega_a (θ = 0):     57.6295 rad/s  [destra del cerchio]
omega_b (θ = π):     60.5800 rad/s  [sinistra del cerchio]
Smorzamento stimato:     η2 = -0.0499

Diametro:    D = 0.000005
Costante modale stimata:     2Ã3,3 = -0.000818
fx >>
```

Figure 3.6 Results for the second modal component

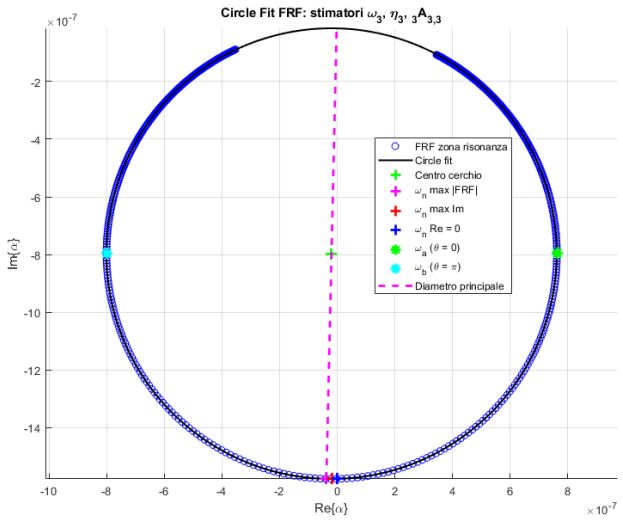

Figure 3.7 Circle-fit for the receptance function around the third peak

```
=== Frequenze naturali stimate sulla circle fit ===
Metodo 1 (max Im):        ω3 = 133.0419 rad/s
Metodo 2 (Re = 0):        ω3  = 133.0017 rad/s
Metodo 3 (max |FRF|):     ω3  = 133.0813 rad/s

omega_a (θ = 0):     129.6967 rad/s  [destra del cerchio]
omega_b (θ = π):     136.3054 rad/s  [sinistra del cerchio]
Smorzamento stimato:     η3 = -0.0497

Diametro:    D = 0.000002
Costante modale stimata:     3A3,3 = -0.001375
>>
```

Figure 3.8 Results for the third modal component

Table 3.3 Comparison of natural frequencies for the first three modes

Mode r	Reference $\omega_{r,\text{ref}}$ [rad/s]	Measured $\omega_{r,\text{mis}}$ [rad/s]	Relative error e_r [%]
1	14.7804	14.7804	0
2	59.1230	59.1231	0
3	133.0418	133.0419	0

Table 3.4 Comparison of modal damping ratios for the first three modes

Mode r	Reference Damping $\eta_{r,\text{ref}}$	Measured Frequency $\omega_{r,\text{mis}}$ [rad/s]	Relative error e_r [%]
1	0.05	0.0499	0.2
2	0.05	0.0501	0.2
3	0.05	0.0497	0.6

Table 3.5 Comparison of modal constants for the first three modes

Mode r	Reference Modal Constant ${}_rA_{3,3,\text{ref}}$	Measured Modal Constant ${}_rA_{3,3,\text{mis}}$	Relative error e_r [%]
1	2.4054×10^{-4}	2.41×10^{-4}	2.1
2	8.2179×10^{-4}	8.18×10^{-4}	0.5
3	1.4000×10^{-3}	1.375×10^{-3}	1.8